



Constraining slip rates along Altay faults using GNSS data

Fabien Ramel¹, Philippe Vernant¹, Jean-François Ritz¹, Erik Doerflinger¹, Erdenezul Danzansan², Dulguun Ayush ², Alain Chauvet¹, Ulzibat Munkhuu², Sodnomsambuu Demberel²

- 1. Lab. Geosiences Montpellier, University Montpellier 2-CNRS, 34095 Montpellier, France
- 2. Institute of Astronomy and Geophysics, Mongolian Academy of Sciences, Ulan Bator, Mongolia

Correspondence to: Fabien Ramel (fabien.ramel@outlook.fr)

Abstract. A first block modeling study of the Mongolian Altay is presented, based on a new GNSS dataset acquired across the range with an innovative setup. Our results show that approximately 4–6 mm.yr⁻¹ of dextral strike-slip motion is accommodated across the ~400 km-wide Altay deformation zone, consistent with previous geodetic estimates. Compared to the more scattered and heterogeneous slip rate estimates from morphotectonic studies, our results provide improved constraints on slip rates along the main Altay faults. Combining knowledge about fault activity across Altay with our results we also discuss the potential role of other unmodeled intra-block structures in accommodating deformation in the Altay and its periphery. This also leads us to question the highest previously reported slip rates—particularly along the Har-Us-Nuur and Fu-Yun faults.

Keyword: GNSS, Slip rates, Active faults, Block model, Kinematic, Altay

1. INTRODUCTION

15

Understanding the mechanisms driving continental deformation across Central Asia has long been a central focus in the field of active tectonics (e.g. Molnar & Tapponier, 1975; Tapponier & Molnar, 1979; Tapponier, 1982; England & Molnar, 1997; Peltzer & Saucier, 1996). While numerous paleoseismological, morphotectonic, and geodetic studies have targeted the major fault systems associated with the Himalayas, Tibetan Plateau, Kunlun, and Tien Shan—directly linked to the India—Asia convergence—regions located farther into the continental interior, such as the Altay and Gobi-Altay ranges, have received comparatively less attention (e.g. Tapponier & Molnar, 1979; Baljinnyam et al., 1993; Cunningham et al., 1996; Cunningham et al., 2010). Yet, the Mongolian Altay and Gobi-Altay represent major intracontinental deformation zones in Central Asia, shaped by large-scale, right-lateral strike-slip fault systems extending over several hundred kilometers and capable of generating large-magnitude earthquakes (e.g. Walker et al., 2007; Klinger et al., 2011; Rizza et al., 2015; Kurtz et al., 2018).

From a geodetic perspective, the region has long suffered from limited GNSS data coverage, preventing the development of detailed studies capable of accurately characterizing fault kinematics and regional strain distribution (Calais et al., 2003, 2006;





Lukhnev et al., 2010, 2025). Since the pioneering studies of Calais et al. (2003), GNSS coverage in the area has remained limited to fewer than five stations, while the Junggar region immediately to the south has undergone a substantial densification of its GNSS network (e.g. Wang and Shen, 2020).

In this study, we present a new kinematic analysis of active deformation across the Mongolian Altay by quantifying the interseismic deformation field and modeling fault slip using a block modeling approach. To this end, we acquired new GNSS data during multiple field campaigns conducted since 2019 along two transects crossing the Altay range. This modeling, based on improved geodetic constraints, allows us to better resolve the regional strain rate field and evaluate fault slip rates through direct comparison with previously published morphotectonic estimates.

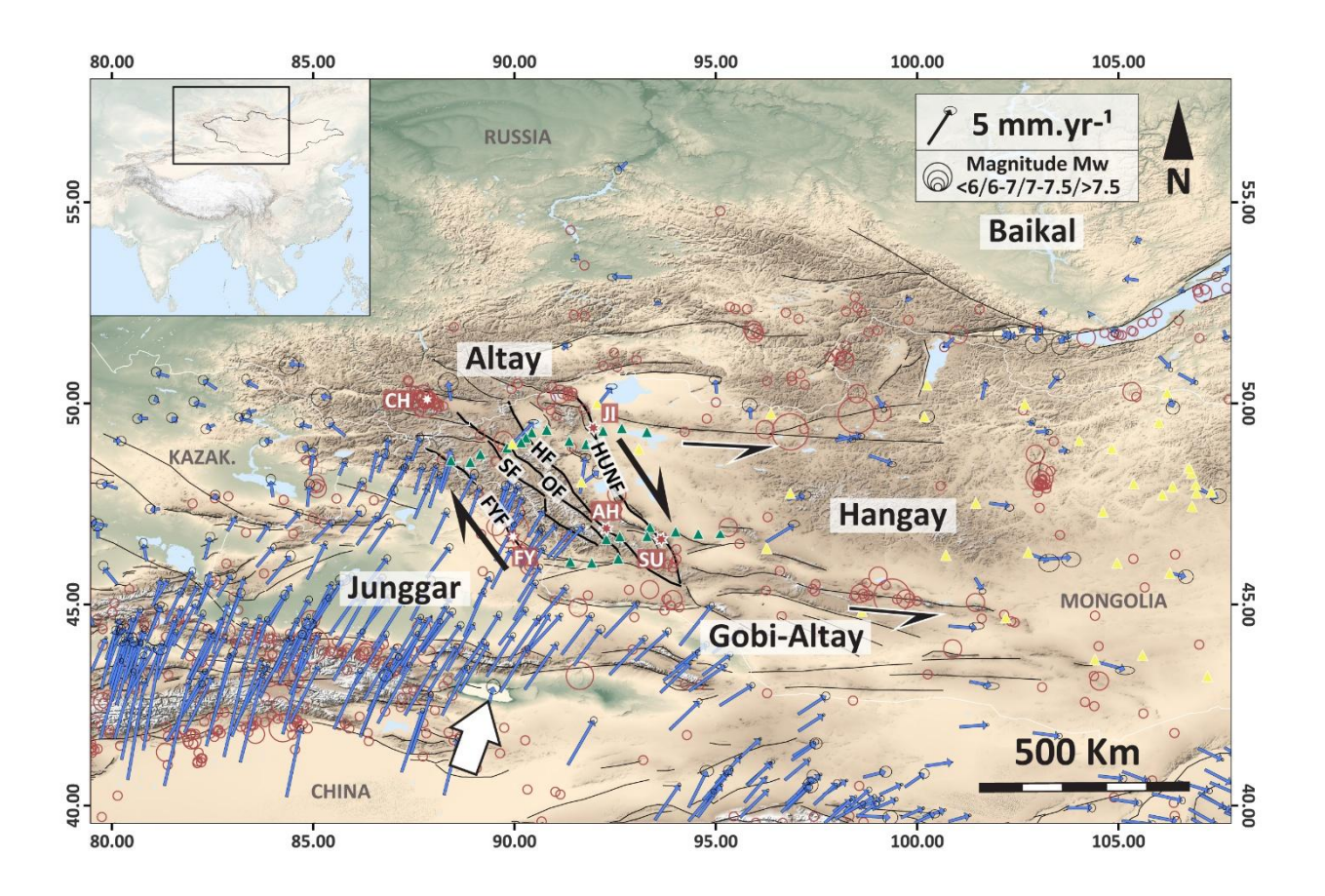


Figure 1. Major active fault systems, seismicity (ISC-GEM Global Instrumental Earthquake Catalogue (1904–2020)), velocity fields (Eurasia-fixed reference frame, (Wang & Shen, 2020; W. Wang et al., 2017)), and GNSS transects used in this study. HUNF: Har-Us-Nuur Fault, HF: Hovd Fault, OF: Ölgiy Fault, FYF: Fu-Yun Fault. Stars correspond to earthquakes (red) and main known





surface ruptures documented (white). Earthquakes: FY: Fu-Yun, Mw=8.0, 1931; CH: Chuya, Mw=7.3, 2003. Known surface ruptures: AR: Ar-Hötöl, SU: Sutai, JI: Jid. The large white arrow indicates the principal stress axis associated with India-Asia convergence. Green triangles represent GNSS measurement sites for the southern and northern transects implemented in this study. Yellow triangles represent continuous permanent stations.

2. TECTONIC SETTING

The Altay massif marks the western boundary of Mongolia, where its relief forms an orographic frontier with Russia to the north and China to the south (Fig. 1). This intracontinental, transpressive mountain range is structured by major right-lateral strike-slip faults, restraining bends, and fault terminations giving rise to positive flower structures (Cunningham et al., 1996, 2003, 2005; Tapponnier & Molnar, 1979). The Altay is regarded as a deformable block sandwiched between the rigid domains of the Siberian platform to the north and the Junggar basin to the south (Cunningham et al., 2005; Huangfu et al., 2023). The ancient NW-SE-oriented tectono-stratigraphic boundaries of Paleozoic units structuring the Altay act as zones of weakness where current deformation is localized (Buslov et al., 2001; Badarch et al., 2002; Sengör et al., 1993; Windley et al., 2007; W. Xiao et al., 2010, 2015, Cunningham et al., 1996, 2003). The tectonic activity in the region is associated with the far-field effects of the India-Asia convergence, which has led to the development of Central Asia's relief, including the Tibetan Plateau, Tien Shan, Altay, and Gobi-Altay, throughout the Cenozoic (Molnar & Tapponnier, 1975; De Grave et al., 2007). To the east, the Hangay dome is interpreted as a rigid block with a Precambrian basement, against which the Altay and Gobi-Altay domains are pushed and deformed (W. D. Cunningham, 2001). Tectonic activity in this region is documented, but the proposed mechanisms—whether lithospheric or asthenospheric in origin—remain debated (Chen et al., 2015a; W. D. Cunningham, 2001; Demouchy et al., 2019; R. Walker et al., 2007; R. T. Walker et al., 2008).

2.1 Active Tectonics in the Mongolia-Baikal Region

The complex kinematics of the Mongolia-Baikal region, where dextral and left-lateral strike-slip and extensional domains coexist—represented by the Altay, Gobi-Altay, and Baikal, respectively—make this area zone of major interest for studying intracontinental deformation in Central Asia (Fig. 1).

The occurrence of four major earthquakes of $Mw \ge 8.0$ during the 20^{th} century in western Mongolia (Baljinnyam et al., 1993) has sparked decades-long debate about the mechanisms driving this exceptional seismicity (Chery et al., 2001; Shao et al., 2024). Over the past 20 years, morphotectonic studies were carried out on the faults of Bolnai (Rizza et al., 2015; Choi et al., 2018), of the Gobi-Altay (Ritz et al., 1995, 2003, 2006; Prentice et al., 2002; Vassallo et al., 2006; Rizza et al., 2011; Kurtz et al., 2018), and Fu-Yun (Klinger et al., 2011; Fan et al., 2022). They revealed the existence of slow faults with slip rates of about 1 mm.yr⁻¹ capable of generating large earthquakes separated by quiescent periods of several thousand years. Based on



80



GPS surveys, Calais et al., (2003, 2006) and Q. Wang et al., (2001) estimated that approximately 10–20% of the shortening induced by the India-Asia convergence is accommodated along the major faults of the Altay.

2.2 Active Tectonics in the Altay

Several studies dated between 20 and 5 million years ago the onset of Altay massif formation linked to the transpressive reactivation of ancient Paleozoic structures (De Grave et al., 2007; De Grave & Van den Haute, 2002; Howard et al., 2003, 2006; Vassallo, 2006; Yuan et al., 2006). Although characterized by moderate seismicity, the Altay experienced two major earthquakes in the last century: the Mw 8.0 Fu-Yun earthquake in 1931 and the more recent Mw 7.3 Chuya earthquake in 2003 in the Russian Altay.

The chain's four main fault systems—Har-Us-Nuur, Hovd, Ölgiy, and Fu-Yun—provide evidence of tectonic activity. Indeed, numerous historical and Holocene surface ruptures have been documented, such as Fu-Yun (Klinger et al., 2011), Ar-Hötöl (Davaasambuu et al., 2022), Jid (Walker et al., 2006) and Sutaï (Ramel et al., 2025). Morphotectonic studies along the Altay's faults, based on absolute dating, have yielded slip rates ranging from 0.5 to 2.8 mm.yr⁻¹. Using terrestrial cosmogenic nuclide (TCN), dating of offset fan surfaces (10 Be), Nissen et al. (2009) estimated a horizontal slip rate of 2.4 ± 0.4 mm.yr⁻¹ along the central section of the Har-Us-Nuur fault over the past 75 kyr while Ramel et al., (2025) calculated a minimum slip rate of 0.32 ± 0.04 mm.yr⁻¹ along the southern section of the fault. Along the Hovd fault, Vassallo (2006), using 10 Be concentrations of surface boulders and depth profiles of fan-terraces, estimated a minimum horizontal slip rate of about 0.5 mm.yr⁻¹ over the past 40–100 kyr for a site on the northern part of the fault and 1.2 ± 0.7 mm.yr⁻¹ over the past 15–40 kyr within its central section. Ha et al., (2023) calculated a horizontal slip rate of $1.8^{+0.8}$ /_{-0.1} mm.yr⁻¹ for the past 25 kyr by analyzing 10 Be concentrations of surface boulders along the central section of the same fault.

For the Ölgiy fault, combining ²³⁸U-²³⁴U-²³⁰Th and ¹⁰Be dating methods, Gregory et al., (2014) found a slip rate of 0.3 – 1.3 mm.yr⁻¹ over the past 20–30 kyr while Frankel et al., (2010) calculated a slip rate of 0.8 – 1.1 mm.yr⁻¹ over the past 15 – 25 kyr using ¹⁰Be concentrations from surface samples. Finally, along the Fu-Yun fault, Xu et al., (2012) and Wu et al., (2024) estimated slip rates of about 1 mm.yr⁻¹ using ¹⁰Be and OSL dating, respectively.

The Sagsay fault system (SF), while exhibiting evidence of significant surface rupturing activity in the north and cumulative displacements in the south (Baljinnyam et al., 1993; Gregory, 2012), has not yet been the subject of slip rate estimations.

These studies remain limited due to the fact they are long to carry out and often suffer from methodological heterogeneity. Thus, when considering all studies based on absolute dating, estimates for the total right-lateral strike-slip component across the Altay range from 2.0 to 9.0 mm.yr⁻¹. A first-order estimate based on GPS data of Calais et al., (2003) provides values between approximately 4 and 7 mm.yr⁻¹ (see Table 1).



120

125

130



HORIZONTAL SLIP RATES BASED ON ABSOLUTE DATING						
Fault system	Segment fault	Min HSR (mm.yr ⁻¹)	Max HSR (mm.yr ⁻¹)	Slip-rate period	Dating method	Reference
Har-Us- Nuur	Sutaï, Jargalant	0.3	2.8	75.0 kyr	¹⁰ Be	Ramel et al., 2025 Nissen et al., 2009
Hovd	Tsambagaraav, Ih Turgen	0.5	2.6	16.1 – 110 kyr	¹⁰ Be	Vassalo, 2006 ; Ha et al., 2023
Ölgiy	Höh Serh	0.8	1.3	15.9 – 70 kyr	¹⁰ Be; ²³⁸ U- ²³⁴ U- ²³⁰ Th Serie and ¹⁰ Be	Frankel., 2010 ; Gregory, 2014
Fu-yun	Fu-yun	0.4	2.3	< 150 kyr	¹⁰ Be ; OSL	Xu et al., 2012 ; Wu et al., 2024
TOTAL HORIZONTAL SLIP RATES ACROSS ALTAY						
From morphotectonics studies		2	9	References above		
From GPS data		3.8	6.6	Calculations based on URUM and ULAA stations from Calais et al., 2003 and on min and max values for Altay fault orientations (315 - 345°)		

Table 1. Summary table of slip rates estimated in the literature based on absolute dating and the total strike-slip displacement across the Altay as derived from morphotectonic and geodetic data.

2.3 Contribution of GNSS Data and Modelling

The GNSS data available for the Altay and Mongolia provided by Calais et al. (2006) are about two decades old and offer limited spatio-temporal coverage, insufficient for accurately modeling deformation within the Altay. More recently, M. Wang & Shen (2020) published a new velocity field synthesizing available data across Central Asia, including additional data from China. However, for our study, these data only improve coverage for the area south of the Altay, in particular the Junggar region.

Over the past decades, several studies based on these data sets and block modeling approaches have been conducted to propose kinematics models of Central Asian deformation. Using around ten blocks to model deformation across the Tibetan Plateau, Thatcher (2007) estimated slip rates on major faults of the region. Y. Wang et al. (2017) and Li et al. (2017) focused on the northern Tibetan region, while Gu et al. (2024) proposed a block model for the Tien Shan, including a block for Junggar. Meade (2007) and W. Wang et al. (2017) modeled fault slip rates by defining blocks encompassing the entire India-Asia region, extending to the Tien Shan in the former and to Siberia in the latter.

W. Wang et al. (2017) defined distinct blocks for the Junggar and Gobi-Altay regions but considered a single Siberia block that encompasses the Altay region and its surroundings. All these studies show that no detailed modeling of Altay fault velocities has been carried out to date. Here, we develop a first block model for the Altay, using blocks delineated by the major fault systems of the region. This allows us to model the interseismic deformation distribution through the Altay range and surrounding regions and to estimate geodetically derived fault slip rates.



135

140

145

150

155



3. GNSS DATA AND ANALYSIS

We acquired new GNSS data over the past five years by installing two transects located to the south and north of the Altay (Fig. 1). The transects consist of 10 and 13 measurement points, respectively, with a mean distance between the sites of approximately 40 kilometers. Two field campaigns conducted in 2019 and 2020 were necessary to setup the sites along the two transects and conduct the firsts surveys.

We designed an innovative setup to enable the precise repositioning of antennas from one campaign to another (Fig. 2a, b). The selected sites for point implantation correspond to stable bedrock outcrops where holes are drilled and can be reused for each measurement. The 8 mm diameter drilled holes are used to anchor a removable and repositionable mounting system (8 mm Petzl pulse) (Fig. 2c). The hanger plate of the Petzl pulse was modified so as to keep only a roughly circular plate laying on the rock (Fig. 2b). The short antenna mast (24.8 cm) tip is positioned in a hole centered at the top of the device. We consider the bottom of the hole on top of the Petzl pulse to be the reference for the height of the site. But we warn that even though this device is accurate for the horizontal positioning, the vertical emplacement suffers from a larger uncertainty related to the surface of the rock surrounding the hole. We choose to use this setup in order to prevent the stealing of permanent benchmarks that we could have glued in the bedrock.

We conducted three measurement campaigns for the southern transect (2019, 2022, 2024) and two for the northern transect (2020, 2023). Measurements were taken over at least 3 UTC days with a minimum of 8 hours of recording the first day, 24h the second one and at least 8 hours the third one.











Figure 2. Repositionable setup for GNSS antenna installation. a: Photo of the antenna mounted on a tripod. b: Photo of the repositionable device in place. c: Photo of the Petzl device used for antenna installation (Petzl).

The survey-mode profiles are complemented by data from the Mongolian continuous GNSS (cGNSS) network, managed by the Mongolian IAG (Institute of Astronomy and Geophysics) (Figure 1). 45 cGNSS sites encompassing a period from the first day of 2015 to the last day of 2024 with time series of at least 2.5 years of complete recording (i.e. at least 912 days of recorded data) were computed.

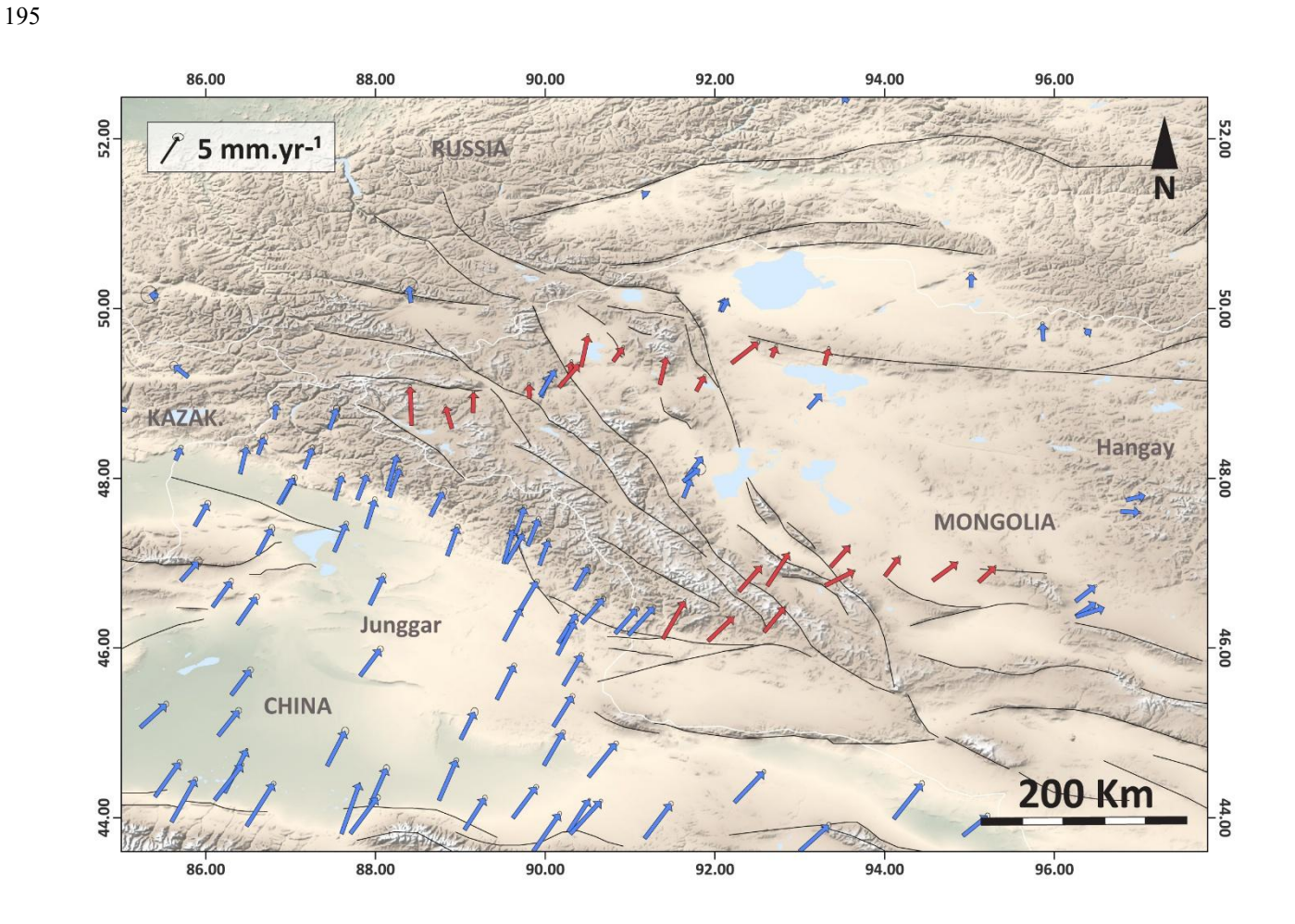
We processed the GNSS data with the Jet Propulsion Laboratory (JPL) GipsyX software (release 1.3) in a Precise Point Positioning mode (Zumberge et al., 1997). We used JPL's final fiducial-free GPS orbit products. Each station data is processed independently insulating it from potential problems at other individual stations. We apply the ambiguity resolution by using the wide lane and phase bias method (Bertiger et al., 2010). We used antenna calibrations from the IGS (Schmid et al., 2007). We also use standard models for tropospheric delay corrections (VMF1, Boehm et al., 2006) and solid Earth and ocean tide loading corrections (FES 2004, Lyard et al., 2006). The daily positions are obtained in IGS14 reference frame. For continuous sites we obtain GNSS velocities and their uncertainties by fitting a linear trend plus annual and semiannual terms and offsets (if needed) to position time series, assuming a white + flicker noise stochastic model (Williams et al. 2003). 175 For survey sites we only fit a linear trend. To have a consistent Eurasia fixed reference frame with Wang and Shen (2020), we align our velocity solution on theirs. We first combined Wang and Shen (2020) velocity solution (including velocities from Kreemer et al., 2014, Ader et al., 2012, Ashurkov et al., 2011, Banerjee et al., 2008, Bettinelli et al., 2006, Calais et al., 2006, Galahaut et al., 2013, Ischuk et al., 2013, Jade et al., 2004, Lukhnev et al., 2010, Mahanta et al., 2012, Mahesh et al., 2012, Maurin et al. 2010, Mukul et al., 2010, Mullick et al., 2009, Paul et al., 2001, Ponraj et al., 2010, Schiffman et al., 2013, 180 Shestakov et al., 2010, Simons et al., 2007, Sol et al. 2007, Yang et al., 2008, Zubovich et al., 2010, Devachandra et al., 2014, Gupta et al., 2015, Marechal et al., 2016) with Lukhnev et al. (2025) solution to have the most complete velocity field for the region. The rms on the velocity residuals for the 32 common sites after alignment is 0.32 mm.yr⁻¹. We processed in the same way to combine our velocity field, the rms on the velocity residuals at the 16 common sites (see supplementary files for the list of sites) is 0.50 mm.yr⁻¹. To define a Junggar-fixed reference frame and express the velocities of our study area relative to 185 one of the blocks bordering the Altay region, we use 39 sites to compute the Junggar/Eurasia Euler pole (75.687°E, 49.929°N, 0.301°/Myr, see supplementary material for the list of sites). Figures 3a and 3b show the calculated velocity fields for the Eurasia-fixed and Junggar-fixed reference frames, respectively (see supplementary for velocity field data). The velocity field for the northern transect reveals more heterogeneous direction and magnitude vectors, likely due to the fact that only two measurements were conducted in this area over a shorter time interval.





The velocity field in the Eurasia-fixed reference frame highlights shortening velocity gradients, particularly along the southern transect (Fig. 3a). The direction of shortening aligns with the orientation of vectors observed farther south in the Tien Shan, where it is interpreted as the far-field effect of India-Asia convergence.

The dextral strike-slip kinematics of Altay faults is especially well illustrated by the velocity gradient observed in the velocity field in the Junggar fixed reference frame (Fig. 3b).







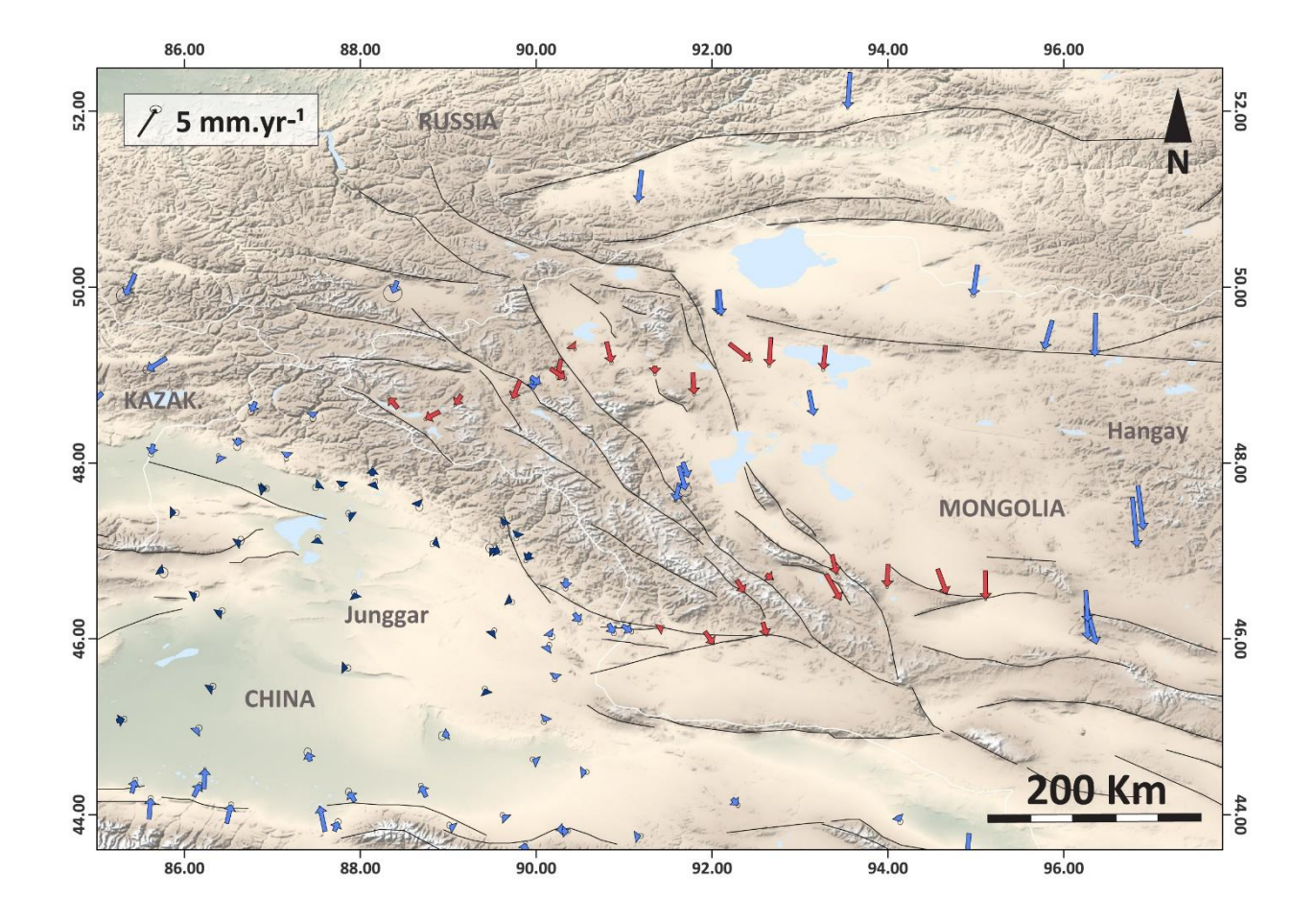


Figure 3. GNSS velocity fields calculated from data compiled by (M. Wang & Shen, 2020) in blue and data acquired in this study in red. a: Eurasia-fixed reference frame. b: Junggar-fixed reference frame. In black are the sites of the velocity field of (M. Wang & Shen, 2020) used to define the Junggar-fixed reference frame.

4. MODELING THE INTERSEISMIC VELOCITY FIELD

Figure 5 shows block boundaries we used to model the interseismic velocity field in terms of relative block motions and associated elastic strain accumulation on block-bounding structures (McCaffrey,2013; Meade and Hager, 2005). Block boundaries are designed from mapped faults, seismicity, historic earthquakes, and the GPS velocities. All faults used in the model must be associated with a block boundary, this implies that no slip on "unconnected" fault segments is allowed, and all





- the blocks must be closed. The models include block rotations on a sphere with elastic strain accumulation on block-bounding faults following the formulation of Okada (1985). Relative block motions (relative Euler vectors) are estimated using the TDEFNODE code (McCaffrey, 2002) by minimizing the GPS residual motions within the blocks in a least squares sense. Fault slip rates are determined by decomposing relative block motions on block boundaries into fault parallel (strike-slip, positive right-lateral) and fault-normal motions (normal and thrust, negative compression).
- The model is centered on the Altay and includes adjacent blocks required for the purpose of modeling. For the Altay region, three blocks are defined: FYUN, HOVD, and HUSN, named after the principal faults separating them. The same coupling and locking depth parameters are used for both models investigated. These parameters imply that all the faults are fully coupled down to a depth of 15 km.
- Two models are explored to assess the potential role of processes associated with the Hangay Dome on regional deformation and their potential impact on Altay's faults activity. The first model uses the standard parameters described above and does not allow internal deformation within the blocks, while the second model allows internal deformation within the MONG block, which largely encompasses the Hangay region.
- Both models exhibit very similar characteristics in terms of residuals and slip rates (Fig. 5b,c). Low residuals are observed along the two transects, although they are slightly higher than those seen in neighboring regions like the Junggar, which benefits from more GNSS data and longer time series. The stronger residuals found along the northern transect compared to the southern transect can be attributed to the limited data of the former, based only on two surveys three years apart.
 - From a kinematic perspective, both models effectively reproduce the right-lateral strike-slip style of the major NW-SE faults in the Altay. The modeled horizontal slip rates are around 0.5 1.5 mm.yr⁻¹ along the majority of the NW-SE oriented fault segments, while higher values are found along the Fu-Yun fault and along the HUN fault in the strain-free model for block MONG, where values reach ~1.5–2.5 mm.yr⁻¹.
 - The main differences between the two models are the slip rates found along the HUN fault. The modeling shows that the NW-SE-oriented internal compressive deformation within the MONG block reduces slip rates along the fault by at least 1 mm.yr⁻¹.
- Modeled fault-normal components show more heterogeneity. Overall, the observed values are below 1 mm.yr⁻¹ or less along the NW-SE major faults. The kinematics are predominantly compressive in the south and west, except along the Ölgiy Fault, while extensional deformation is observed in the north. However, the very low extensive values (< 0.5 mm.yr⁻¹) found along this fault are not significant and prevent any conclusion on the possible normal component of the fault.
- Notable differences are observed between the major NW-SE structures of the Altay and the E-W-oriented northern fault terminations. Slip rates are generally higher along these terminations, especially for the normal fault components reaching up to more than 3-4 mm.yr⁻¹, particularly at the terminations of the HUN and Hovd faults. The left-lateral kinematics observed in these regions highlight a limitation of the models and the GNSS dataset, and may be attributed to the very limited GNSS





coverage of this area. Consequently, the relative movements of the Altay blocks with respect to the SIBE block are poorly constrained.

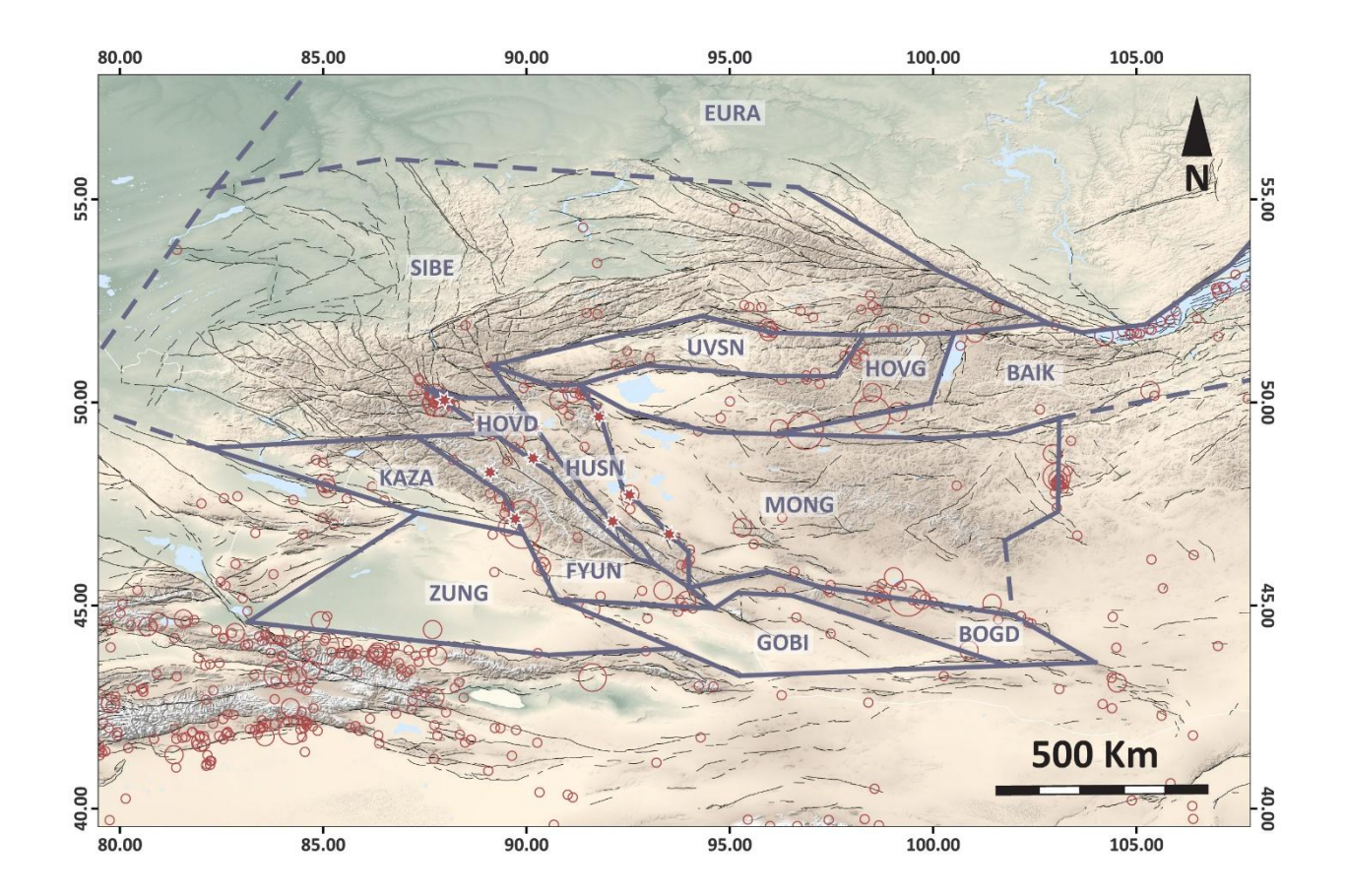
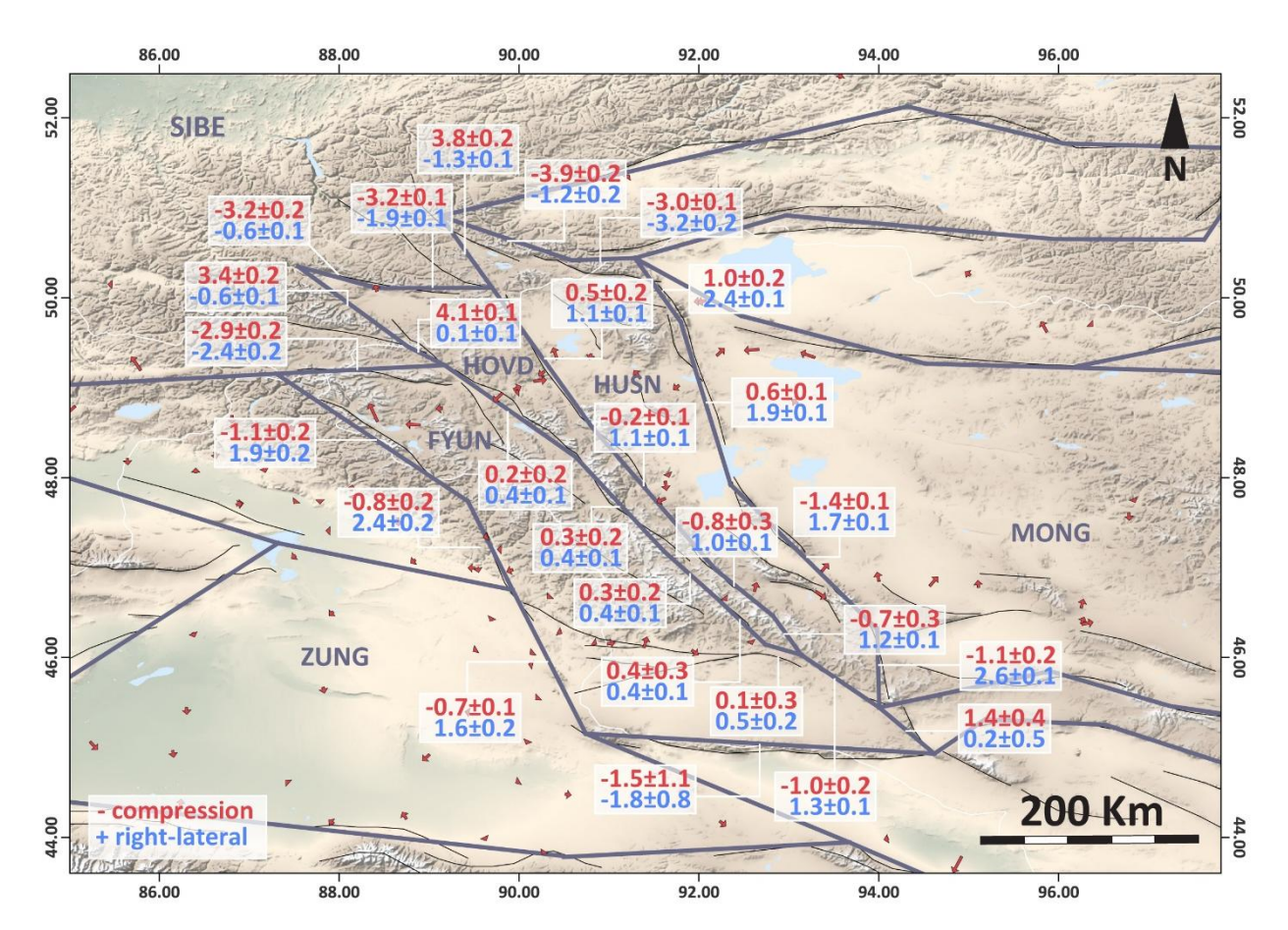


Figure 4. Seismotectonic map of the Mongolian-Altay region used for block modeling. Gray polygons represent blocks defined for modeling. Dashed lines represent either poorly constrained block boundaries or artificial boundaries introduced to close block polygons. Thin black lines correspond to potentially active faults from the Eurasian Active Fault Database (Zelenin et al., 2022). Red circles indicate instrumental seismicity from the International Seismological Centre (ISC) catalog (accessed 2025). Red stars point out known surface ruptures in the Altay range.











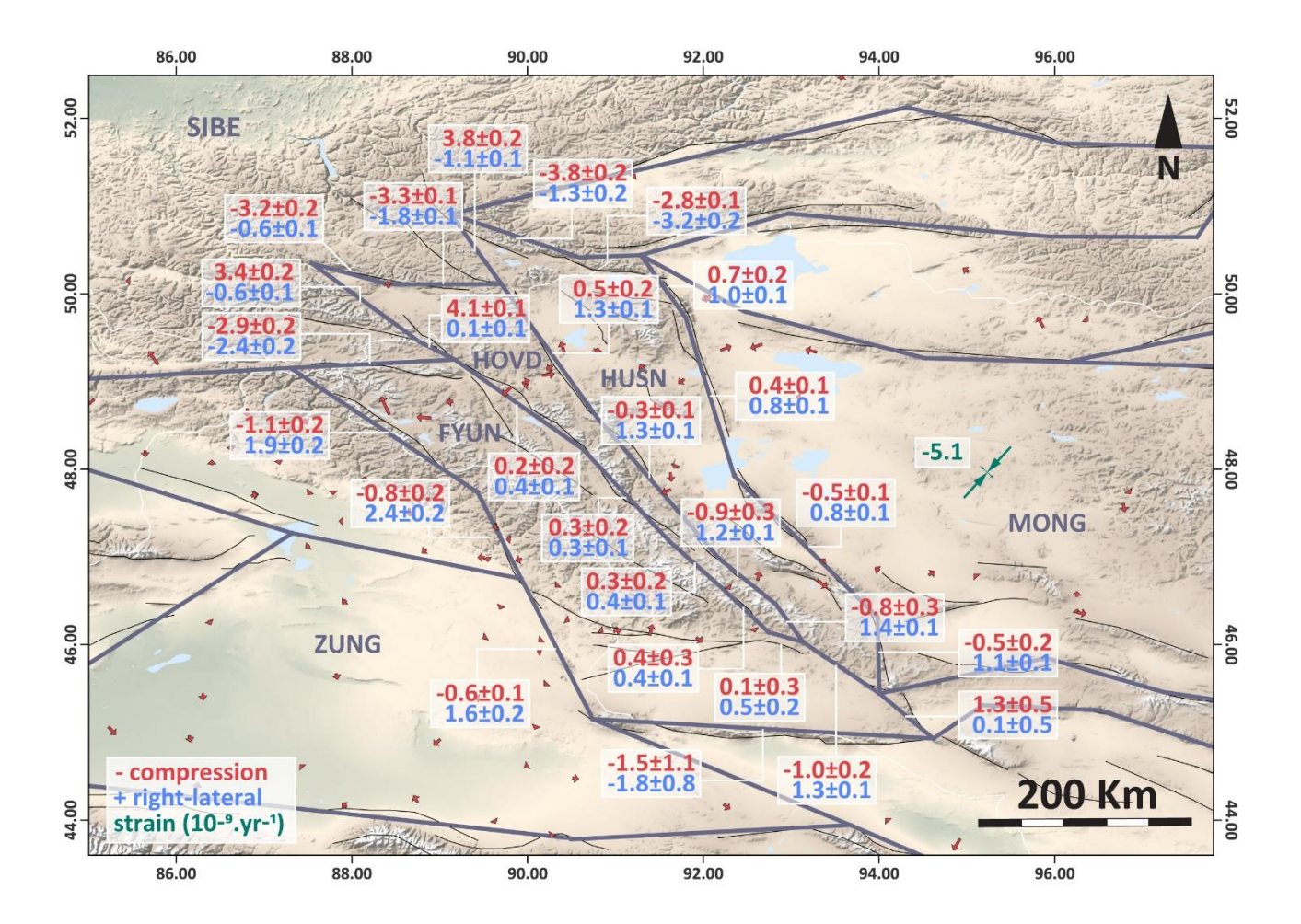


Figure 5. Block model results. The map shows the geometry of the block model, residual velocities, modeled slip rates (blue: fault-parallel component, red: normal fault component), and strain. a. Block model with standard parameters. b. Block model including strain in the MONG block. Formal uncertainty provided by the TDEFNODE software (McCaffrey, 2002) are provided at 1σ level confidence interval, but Karakhanyan et al. (2013) from an extensive study suggested that realistic uncertainties are more on the order of 0.8-1 mm/yr.

5. DISCUSSION

265

270

5.1 Kinematic Analysis

Our study extends the characterization of the kinematics of intracontinental deformation in Central Asia. By focusing on the Altay region, we clarify the interactions between the major lithospheric blocks of one of the key areas of intracontinental deformation, located at the junction between the India-Asia convergence zone and the stable Siberian craton. The new GNSS





dataset acquired through the implementation of two GNSS transects provides improved geodetic coverage of the region.

Moreover, our study demonstrates the potential of conducting short-term GNSS campaigns in areas characterized by low deformation rates and the efficiency of our repositionable measurement device for such acquisitions. Our block model provides the first detailed GNSS kinematic description of Altay deformation, with the following important observations:

From a kinematic perspective, the geomorphological right-lateral strike-slip motion observed along the major NW–SE faults in the Altay region is well reproduced by our model. However, the modeled fault-normal components reveal contrasting behaviors between the southern and northern segments. Compression is modeled along the southern faults, whereas extension is observed in the north and along the Ölgiy fault. This modeled extension decreases when deformation is allowed in the MONG block. This suggests that this extension might be related to unaccounted for deformation due to the limited GNSS network coverage along the northern transect. As the blocks in the Altay are narrow and elongated, uncertainties in the GNSS velocities can easily induce a lever arm effect producing slight extension or compression where most of the deformation might only be strike-slip. Without longer time series allowing better GNSS velocity estimates we cannot conclude whether or not this extension should be considered as significant.

290 The fault terminations located north of the Altay, as well as the fault bounding FYUN block—generally oriented E–W—exhibit sinistral kinematics in our model. For the northern fault terminations, this kinematic behavior is not consistent with geomorphological evidence (e.g., Cunningham et al., 2003; Bayasgalan et al., 1999). However, the strong compressive components modeled along these structures align well with the positive flower structures observed in the field. The sinistral fault-parallel motion modeled along the segment corresponding to the Chuya fault, located north of the Ölgiy fault system, also appears inconsistent with the documented right-lateral displacement associated with the 2003 earthquake. However, the very low magnitude of this component—approximately 0.5 mm.yr⁻¹—and the near-zero value observed along the immediately adjacent segment to the south, which moreover exhibits an opposite (right-lateral) kinematic, suggest that the discrepancy is minor and likely reflects modeling uncertainties more likely related to the narrow and elongated block geometries. Similarly, the high normal fault component modeled is incompatible with the observed oblique-slip mechanisms of the 2003 Chuya earthquake sequence, which predominantly exhibit right-lateral strike-slip motion combined with reverse faulting (Nissen et al., 2007).

The model including internal deformation within the MONG block shows only few differences compared to the standard model. Indeed, in this configuration, residuals are slightly lower within the MONG block while slip rates are reduced by more than 1 mm.yr⁻¹ along the Har-Us-Nuur fault system. The lower residuals suggest that deformation occurs within the MONG block with the implication of reducing the slip rate on the HUN fault. However, GNSS coverage for this block remains too



330



scarce to allow us to determine if the deformation is distributed as in the current model or if it should be localized on a major structure within the MONG block by splitting it in smaller blocks.

310 Several studies have documented active faults around and within the Hangay region, structures that could accommodate some deformation. Cunningham (2001) documented numerous normal faults, mostly NE-SW oriented. Walker et al. (2007) highlighted a large sinistral active fault system south of the Hangay dome. Based on their observations, they showed that the normal faults south of Hangay connect to this structure as releasing bends. They pointed out that in this context, the kinematics of active faults in the region are consistent with the shearing deformation field observed from GNSS data in the center of 315 Mongolia. More recently, Walker et al., (2017) documented a major surface rupture along a normal fault southwest of Hangay dome with limited cumulative displacement and low slip rates, noting that such deformation is likely undetectable by all but the longest-operating GPS networks. Van der Wal et al. (2021) also documented an active transpressive sinistral fault system in the valley of the Great Lakes south of Hangay, suggesting deformation along previously unknown faults. These studies highlight various expressions of sinistral transpressive kinematics in the region and their connection with inherited structures. 320 The internal deformation suggested by our model within the MONG block supports these findings. Indeed, the orientation of the maximum compressive strain axis (NE-SW) is compatible with sinistral kinematics along EW structures and either extensional or compressive deformation along NE-SW and NW-SE faults, respectively. Nevertheless, the origin of the current tectonics in the Hangay region remains debated. It has been associated with a process of doming, and different lithospheric or asthenospheric mechanisms have been proposed (Demouchy et al., 2019; Barruol et al., 2008; Chen et al., 2015b; W. D. Cunningham, 1998, 2001) without reaching a consensus. 325

5.2 Slip Rates Estimates and Comparison with Geological Studies

Our modeling also provides estimates of slip rates along the Altay faults. To evaluate the total horizontal slip across the Altay, we sum the modeled minimum and maximum slip rates—accounting for associated uncertainties—along segments of the major NW–SE-trending Altay faults. Considering all models and transects, this yields a total estimated slip rate ranging between 4 and 6 mm.yr⁻¹. These values confirm the preliminary estimates made two decades ago by Calais et al. (2003) and allow us to further discuss the geological data on the different Altay faults.

If the deformation was evenly distributed across the four main fault systems of the Altay (HUNF, HF, OF, FYUF), our GNSS results would yield slip rates of approximately 1 to 1.5 mm.yr⁻¹ per fault, but our models suggest otherwise.

For the Fu-Yun fault system, slip rates are the same for both models with the highest strike-slip rate reported for the central segment (2.4 mm.yr⁻¹), while the northern one has an intermediate rate (1.9 mm.yr⁻¹) and the southern one the lowest rate with 1.6 mm.yr⁻¹. It implies that a significant portion of the regional deformation is accommodated by this fault. Unfortunately, due to the heterogeneity of slip-rate estimates from morphotectonic studies, it is difficult to compare them directly with our



345

350

355

360

365

370



results. Furthermore, part of the modeled deformation along Fu-Yun might be distributed across other structures. The Sagsay fault system is a likely candidate (Fig.1). This lesser-known system exhibits numerous markers of recent activity, notably the surface rupture of the same name to the north and various morphotectonic markers along the system's southern extent (Baljinnyam et al., 1993; Gregory, 2012). Sadly, the GNSS coverage in this area is too scarce and prevents the modeling of an additional block defined by the Sagsay fault system to estimate its potential role. It is also better to have larger blocks to properly estimate their motion, and the elastic strain related to their boundaries. These conditions are not fulfilled in this case. This highlights the importance of conducting morphotectonic studies along this fault system in the future to better characterize its contribution to the regional deformation.

As for Fu-Yun fault, the Ölgiy fault has the same slip-rates, independently from the model. The estimated strike-slip rates for segments belonging to the Ölgiy fault are fairly constant around 0.4 mm.yr⁻¹. This suggests that the Ölgiy fault has the lowest slip-rates of the modeled faults in the Altay. This is not in agreement with the reported morphotectonic slip rates which range from 0.8 to 1.3 mm.yr⁻¹. But one should notice that given the uncertainties this discrepancy is barely significant.

For the Hovd fault, the modeled slip rates vary depending on the model, but the variations are not significant with a difference of +0.2 mm.yr⁻¹ for the model where the MONG block has internal deformation. The estimated slip rates are on the order of 1.1 or 1.3 mm.yr⁻¹. This is definitely lower than the morphotectonic estimate of 2.6 mm.yr⁻¹ (Ha et al., 2023), but close from the 0.5 mm.yr⁻¹ proposed by Vassalo (2006). Given the narrowness of the HOVD block, the total geodetic slip rate across the Ölgiy and Hovd faults (~1.5 mm.yr⁻¹) is similar to the lower morphotectonic estimate (~1.5 mm.yr⁻¹).

For the HUN faults, the strike-slip rates are divided by about two when internal deformation is allowed for the MONG block, hence, the strike-slip rates vary between 1.7 and 2.6 mm.yr $^{-1}$ (no internal deformation) or 0.8 and 1.1 mm.yr $^{-1}$ (internal deformation). Morphotectonic slip rates range from 0.3 mm.yr $^{-1}$ (Ramel et al., 2025) to 2.8 mm.yr $^{-1}$ (Nissen et al., 2009). For both models, the estimated slip rates along the segment studied by Nissen et al. (2009) are systematically lower (1.7 \pm 0.1 mm.yr $^{-1}$ or 0.8 \pm 0.1 mm.yr $^{-1}$ with or without internal deformation, respectively). The geomorphic evidence of fault activity along the major fault systems of the Altai does not support the dominance of any single structure in accommodating the regional deformation. All these faults exhibit multiple surface rupture traces that have been dated or interpreted as Holocene in age (Gregory, 2012). A slip rate of approximately 2.5 mm.yr $^{-1}$ for the HUN fault alone would mean that it accounts for between 40 and 60% of the total strike slip across the Altay, which seems unlikely. This leads us to consider the slip rates obtained by Nissen et al., (2009a) as too high. Usually, GNSS derived slip rates are consistent with morphotectonic ones (e.g. Vernant, 2015). Specific cases have reported variations of slip rates but based on short time periods, which could lead to differences with the GNSS estimates (e.g., Weldon et al., 2002; Ferry et al., 2011). In the case of the HUN fault it does not seem to be the case, which calls for a re-examination of the HUN slip rate.

The higher compressive slip rates observed south of the Hovd and HUN faults—particularly in the model without internal deformation—compared to those in the north and along the Ölgiy fault system, which are also kinematically distinct, is a noteworthy feature. One possible explanation lies in the role of the Zereg and Tsetseg faults documented as active by Nissen





et al., (2009b). These faults, located within the HUSN block, are not used in the model; as a result, their contribution to the overall deformation is likely redistributed onto the bounding faults of the block, namely the HUN and Hovd faults.

6. CONCLUSION

380

385

390

395

400

405

The new GNSS dataset acquired along two transects across the Mongolian Altay represents a significant improvement in the geodetic coverage of this region, with over 20 new measurement sites established using a novel, repositionable setup. This technique has proven to be efficient and reliable over a short observation window and offers great potential for future remeasurements that will increase the precision of the velocity field.

Our study presents the first block model focused on the Altay, enabling a refined analysis of the kinematics of intracontinental deformation in western Mongolia. The model highlights a distributed dextral strike-slip deformation of approximately 4–6 mm.yr⁻¹ across a ~300–400 km-wide deformation zone, in line with previous first-order GPS estimates by Calais et al. (2003, 2006). This implies slip rates along the four major fault systems (Har-Us-Nuur, Hovd, Ölgiy, and Fu-Yun) on the order of 1–1.5 mm.yr⁻¹.

These results also provide a valuable comparison point with geological estimates derived from morphotectonic studies. While some geological slip rates reach values as high as 2.8 mm.yr⁻¹ (e.g., Har-Us-Nuur fault), our results suggest that such high values may be overestimated. The model that allows for internal deformation within the central Mongolian (MONG) block is characterized by lower residuals and yields lower fault slip rates for HUN fault that are more consistent with the average Altay's fault slip rates. This suggests that part of the deformation modeled along the HUN fault is potentially distributed along other active faults within the Hangay Dome and surrounding areas.

Moreover, this work underlies the role of lesser known Altay intra-block structures such as the Zereg, Tsetseg and Sagsay faults in accommodating deformation and the need for targeted geological studies along them.

The differences between geological slip rates and those modeled from GNSS data highlight the importance of integrating morphotectonic and geodetic approaches to achieve more accurate quantification of deformation in slowly deforming regions. Future efforts combining GNSS monitoring with detailed geomorphological investigations will be essential to refine models of strain distribution and fault slip in this tectonically active yet poorly instrumented region of Central Asia.

Acknowledgments. This study was carried out in the framework of CNRS PICS 2019 cooperation project "SEISMONG": Strong earthquakes (M>7.5) and interactions between large active faults in Mongolia (PI J-F. Ritz) and the CNRS 2023–2024 International Emerging Action (IEA) proposal « ALTAY»: Analysis and modeling the active tectonics in Altay (PI J-F. Ritz).





Authors are very grateful for the logistical and technical support that was provided during the field trips by the Institute of Astronomy and Geophysics of the Academy of Sciences of Mongolia.

Data availability. The GNSS velocity fields is available in the Supplement to this article.

- 410 Author contribution. Fabien Ramel, Philippe Vernant and Jean-François Ritz designed the study and wrote the initial draft. Erik Doerflinger and Philippe Vernant processed the GNSS data and computed the velocity field. Erdenezul Danzansan and Dulguun Ayush carried out field measurements. Alain Chauvet assisted with data acquisition. Ulzibat Munkhuu and Sodnomsambuu Demberel managed and contributed to data acquisition from the Mongolian cGNSS network.
- 415 **Competing interests.** The authors declare that they have no conflict of interest.

References

- Badarch, G., Cunningham, W., and Windley, B.: A new terrane subdivision for Mongolia: Implications for the Phanerozoic 420 crustal growth of Central Asia, Journal of Asian Earth Sciences, 21, 87-110, https://doi.org/10.1016/S1367-9120(02)00017-2, 2002.
 - Baljinnyam, I., Bayasgalan, A., Borisov, B. A., Cisternas, A., Dem'yanovich, M. G., Ganbaatar, L., Kochetkov, V. M., Kurushin, R. A., Molnar, P., Philip, H., and Vashchilov, Yu. Ya.: Ruptures of Major Earthquakes and Active Deformation in Mongolia and Its Surroundings, in: Geological Society of America Memoirs, vol. 181, Geological Society of America, 1–60,
- https://doi.org/10.1130/MEM181-p1, 1993. Barruol, G., Deschamps, A., Déverchère, J., Mordvinova, V. V., Ulziibat, M., Perrot, J., Artemiev, A. A., Dugarmaa, T., and Bokelmann, G. H. R.: Upper mantle flow beneath and around the Hangay dome, Central Mongolia, Earth and Planetary Science Letters, 274, 221–233, https://doi.org/10.1016/j.epsl.2008.07.027, 2008.
 - Bayasgalan, A.: Active tectonics of Mongolia., Thesis, University of Cambridge, https://doi.org/10/251670, 1999.
- Bertiger, W., Desai, S., Haines, B., Harvey, N., Moore, A., Owen, S., and Weiss, J.: Single receiver phase ambiguity resolution 430 with GPS data, Journal of Geodesy, 84, 327-337, https://doi.org/10.1007/s00190-010-0371-9, 2010. Boehm, J., Werl, B., and Schuh, H.: Troposphere mapping functions for GPS and very long baseline interferometry from European Centre for Medium-Range Weather Forecasts operational analysis data, J. Geophys. Res., 111, 2005JB003629,
 - https://doi.org/10.1029/2005JB003629, 2006.
- Buslov, M. M., Safonova, I., T., W., Obut, O., Y., F., K., I., Semakov, N., Y., S., Smirnova, L., Kazansky, A. Y., and Itaya, 435 T.: Evolution of the Paleo-Asian Ocean (Altai-Sayan Region, Central Asia) and collision of possible Gondwana-derived





- terranes with the southern marginal part of the Siberian continent, Geosciences Journal, 5, https://doi.org/10.1007/BF02910304, 2001.
- Calais, E., Vergnolle, M., San'kov, V., Lukhnev, A., Miroshnitchenko, A., Amarjargal, S., and Déverchère, J.: GPS measurements of crustal deformation in the Baikal-Mongolia area (1994–2002): Implications for current kinematics of Asia, Journal of Geophysical Research: Solid Earth, 108, https://doi.org/10.1029/2002JB002373, 2003.
 - Calais, E., Dong, L., Wang, M., Shen, Z.-K., and Vergnolle, M.: Continental deformation in Asia from a combined GPS solution, Geophysical Research Letters, 33, https://doi.org/10.1029/2006GL028433, 2006.
- Chen, M., Niu, F., Liu, Q., and Tromp, J.: Mantle-driven uplift of Hangai Dome: New seismic constraints from adjoint tomography, Geophysical Research Letters, 42, 6967–6974, https://doi.org/10.1002/2015GL065018, 2015.
 - Chéry, J., Carretier, S., and Ritz, J.-F.: Postseismic stress transfer explains time clustering of large earthquakes in Mongolia, Earth and Planetary Science Letters, 194, 277–286, https://doi.org/10.1016/S0012-821X(01)00552-0, 2001.
 - Choi, J., Klinger, Y., Ferry, M., Ritz, J., Kurtz, R., Rizza, M., Bollinger, L., Davaasambuu, B., Tsend-Ayush, N., and Demberel, S.: Geologic Inheritance and Earthquake Rupture Processes: The 1905 M ≥ 8 Tsetserleg-Bulnay Strike-Slip Earthquake
- 450 Sequence, Mongolia, JGR Solid Earth, 123, 1925–1953, https://doi.org/10.1002/2017JB013962, 2018.
 - Cunningham, D.: Active intracontinental transpressional mountain building in the Mongolian Altai: Defining a new class of orogen, Earth and Planetary Science Letters, 240, 436–444, https://doi.org/10.1016/j.epsl.2005.09.013, 2005.
 - Cunningham, D.: Tectonic setting and structural evolution of the Late Cenozoic Gobi Altai orogen, https://doi.org/10.1144/SP338.17, 2010.
- Cunningham, D., Windley, B. F., Dorjnamjaa, D., Badamgarov, G., and Saandar, M.: A structural transect across the Mongolian Western Altai: Active transpressional mountain building in central Asia, Tectonics, 15, 142–156, https://doi.org/10.1029/95TC02354, 1996.
 - Cunningham, D., Dijkstra Arjan, H., Howard, J., Quarles, A., and Badarch, G.: Active intraplate strike-slip faulting and transpression uplift in the Mongolian Altai, Geological Society Special Publications, 210, 65–87, 2003.
- Cunningham, W. D.: Lithospheric controls on late Cenozoic construction of the Mongolian Altai, Tectonics, 17, 891–902, https://doi.org/10.1029/1998TC900001, 1998.
 - Cunningham, W. D.: Cenozoic normal faulting and regional doming in the southern Hangay region, Central Mongolia: implications for the origin of the Baikal rift province, Tectonophysics, 331, 389–411, https://doi.org/10.1016/S0040-1951(00)00228-6, 2001.
- Davaasambuu, B., Ferry, M., Ritz, J.-F., and Munkhuu, U.: The Ar-Hötöl surface rupture along the Khovd fault (Mongolian Altay), Journal of Maps, 1–9, https://doi.org/10.1080/17445647.2022.2132884, 2022.
 - De Grave, J. and Van den haute, P.: Denudation and cooling of the Lake Teletskoye Region in the Altai Mountains (South Siberia) as revealed by apatite fission-track thermochronology, Tectonophysics, 349, 145–159, https://doi.org/10.1016/S0040-1951(02)00051-3, 2002.

Geosystems, 20, 183–207, https://doi.org/10.1029/2018GC007931, 2019.



475

480



- 470 De Grave, J., Buslov, M. M., and haute, P.: Distant effects of India–Eurasia convergence and Mesozoic intracontinental deformation in Central Asia: Constraints from apatite fission-track thermochronology, Journal of Asian Earth Sciences, 29, 188–204, https://doi.org/10.1016/j.jseaes.2006.03.001, 2007.
 - Demouchy, S., Tommasi, A., Ionov, D., Higgie, K., and Carlson, R. W.: Microstructures, Water Contents, and Seismic Properties of the Mantle Lithosphere Beneath the Northern Limit of the Hangay Dome, Mongolia, Geochemistry, Geophysics,
- England, P. and Molnar, P.: The field of crustal velocity in Asia calculated from Quaternary rates of slip on faults, Geophysical Journal International, 130, 551–582, https://doi.org/10.1111/j.1365-246X.1997.tb01853.x, 1997.
 - Fan, J., Xu, H., Shi, W., Guo, Q., Zhang, S., Wei, X., Cai, M., Huang, S., Wang, J., and Xiao, J.: A ~28-kyr Continuous Lacustrine Paleoseismic Record of the Intraplate, Slow-Slipping Fuyun Fault in Northwest China, Frontiers in Earth Science, 10, 2022.
 - Ferry, M., Abou Karaki, N., Al-Taj, M., and Khalil, L.: Episodic behavior of the Jordan Valley section of the Dead Sea fault from a 14-kyr-long integrated catalogue of large earthquakes, Bulletin of the Seismological Society of America, 101, 39–67, 2011.
- Frankel, K. L., Wegmann, K. W., Bayasgalan, A., Carson, R. J., Bader, N. E., Adiya, T., Bolor, E., Durfey, C. C., Otgonkhuu,
 J., Sprajcar, J., Sweeney, K. E., Walker, R. T., Marstellar, T. L., and Gregory, L.: Late Pleistocene slip rate of the Höh Serh-
- Tsagaan Salaa fault system, Mongolian Altai and intracontinental deformation in central Asia: Mongolian Altai late Pleistocene slip rate, Geophysical Journal International, 183, 1134–1150, https://doi.org/10.1111/j.1365-246X.2010.04826.x, 2010.
 - Gregory, L. C.: Active faulting and deformation of the Mongolian Altay Mountains, Ph.D., University of Oxford, 2012.
 - Gregory, L. C., Thomas, A. L., Walker, R. T., Garland, R., Mac Niocaill, C., Fenton, C. R., Bayasgalan, A., Amgaa, T.,
- Gantulga, B., Xu, S., Schnabel, C., and West, A. J.: Combined uranium series and 10Be cosmogenic exposure dating of surface abandonment: A case study from the Ölgiy strike-slip fault in western Mongolia, Quaternary Geochronology, 24, 27–43, https://doi.org/10.1016/j.quageo.2014.07.005, 2014.
- Gu, C., Zhao, B., Sheng, T., Wang, W., Wang, D., Liu, D., Li, J., Lv, P., and Qiao, X.: The present-day kinematics of the Tianshan orogenic belt constrained by GPS velocities, Geodesy and Geodynamics, https://doi.org/10.1016/j.geog.2024.04.004,
 2024.
 - Ha, S., Seong, Y. B., and Son, M.: Tectonic geomorphology and Quaternary fault slip rates in the Tsambagarav Massif, Mongolian Altai, Earth Surface Processes and Landforms, n/a, https://doi.org/10.1002/esp.5558, 2023.
 - Howard, J. P., Cunningham, W. D., Davies, S. J., Dijkstra, A. H., and Badarch, G.: The stratigraphic and structural evolution of the Dzereg Basin, western Mongolia: clastic sedimentation, transpressional faulting and basin destruction in an intraplate, intracontinental setting, Basin Research, 15, 45–72, https://doi.org/10.1046/j.1365-2117.2003.00198.x, 2003.
 - Howard, J. P., Cunningham, W. D., and Davies, S. J.: Competing processes of clastic deposition and compartmentalized inversion in an actively evolving transpressional basin, western Mongolia, Journal of the Geological Society, 163, 657–670, https://doi.org/10.1144/0016-764904-073, 2006.





- Huangfu, P., Fan, W., Li, Z.-H., Zhang, H., Zhao, J., and Shi, Y.: Linkage between the India–Asia collision and far-field reactivation of the Altai mountains, Palaeogeography, Palaeoclimatology, Palaeoecology, 616, 111478, https://doi.org/10.1016/j.palaeo.2023.111478, 2023.
 - Karakhanyan, A., Vernant, P., Doerflinger, E., Avagyan, A., Philip, H., Aslanyan, R., Champollion, C., Arakelyan, S., Collard, P., Baghdasaryan, H., Peyret, M., Davtyan, V., Calais, E., and Masson, F.: GPS constraints on continental deformation in the Armenian region and Lesser Caucasus, Tectonophysics, 592, 39–45, https://doi.org/10.1016/j.tecto.2013.02.002, 2013.
- Klinger, Y., Etchebes, M., Tapponnier, P., and Narteau, C.: Characteristic slip for five great earthquakes along the Fuyun fault in China, Nature Geoscience, 4, 389–392, https://doi.org/10.1038/ngeo1158, 2011.
 - Kurtz, R., Klinger, Y., Ferry, M., and Ritz, J.-F.: Horizontal surface-slip distribution through several seismic cycles: The Eastern Bogd fault, Gobi-Altai, Mongolia, Tectonophysics, 734–735, 167–182, https://doi.org/10.1016/j.tecto.2018.03.011, 2018.
- Li, Y., Shan, X., Qu, C., Zhang, Y., Song, X., Jiang, Y., Zhang, G., Nocquet, J.-M., Gong, W., Gan, W., and Wang, C.: Elastic block and strain modeling of GPS data around the Haiyuan-Liupanshan fault, northeastern Tibetan Plateau, Journal of Asian Earth Sciences, 150, 87–97, https://doi.org/10.1016/j.jseaes.2017.10.010, 2017.
 - Lukhnev, A. V., San'kov, V. A., Miroshnichenko, A. I., Ashurkov, S. V., and Calais, E.: GPS rotation and strain rates in the Baikal–Mongolia region, Russian Geology and Geophysics, 51, 785–793, https://doi.org/10.1016/j.rgg.2010.06.006, 2010.
- 520 Lukhnev, A. V., Sankov, V. A., Miroshnichenko, A. I., Byzov, L. M., Sankov, A. V., and Lukhneva, O. F.: Velocities and strain rates in the Baikal-Mongolia region from the GNSS data, Journal of Asian Earth Sciences, 281, 106500, https://doi.org/10.1016/j.jseaes.2025.106500, 2025.
 - Lyard, F., Lefevre, F., Letellier, T., and Francis, O.: Modelling the global ocean tides: modern insights from FES2004, Ocean Dynamics, 56, 394–415, https://doi.org/10.1007/s10236-006-0086-x, 2006.
- Masson, C., Mazzotti, S., Vernant, P., and Doerflinger, E.: Extracting small deformation beyond individual station precision from dense GNSS networks in France and Western Europe, Solid Earth Discussions, 1–34, https://doi.org/10.5194/se-2019-89, 2019.
 - Mccaffrey, R.: Crustal Block Rotations and Plate Coupling, in: Geodynamics Series, edited by: Stein, S. and Freymueller, J. T., American Geophysical Union, Washington, D. C., 101–122, https://doi.org/10.1029/GD030p0101, 2013.
- Meade, B.: Present-day Kinematics at the India-Asia collision zone, Geology, 35, https://doi.org/10.1130/G22924A.1, 2007.
 Meade, B. and Hager, B.: Block Models of Crustal Motion in Southern California Constrained by GPS Measurements, J. Geophys. Res., 110, https://doi.org/10.1029/2004JB003209, 2005.
 - Molnar, P. and Tapponnier, P.: Cenozoic Tectonics of Asia: Effects of a Continental Collision: Features of recent continental tectonics in Asia can be interpreted as results of the India-Eurasia collision, Science, 189, 419–426,
- 535 https://doi.org/10.1126/science.189.4201.419, 1975a.



555



- Molnar, P. and Tapponnier, P.: Cenozoic Tectonics of Asia: Effects of a Continental Collision: Features of recent continental tectonics in Asia can be interpreted as results of the India-Eurasia collision, Science, 189, 419–426, https://doi.org/10.1126/science.189.4201.419, 1975b.
- Nissen, E., Walker, R., Molor, E., Fattahi, M., and Bayasgalan, A.: Late Quaternary rates of uplift and shortening at Baatar 540 Hyarhan (Mongolian Altai) with optically stimulated luminescence, Geophysical Journal International, 177, 259–278, https://doi.org/10.1111/j.1365-246X.2008.04067.x, 2009a.
 - Nissen, E., Walker, R. T., Bayasgalan, A., Carter, A., Fattahi, M., Molor, E., Schnabel, C., West, A. J., and Xu, S.: The late Quaternary slip-rate of the Har-Us-Nuur fault (Mongolian Altai) from cosmogenic ¹⁰Be and luminescence dating, Earth and Planetary Science Letters, 286, 467–478, https://doi.org/10.1016/j.epsl.2009.06.048, 2009b.
- Okada, Y.: Surface deformation to shear and tensile faults in a halfspace, Bulletin of the Seismological Society of America, 75, 1985.
 - Peltzer, G. and Saucier, F.: Present-day kinematics of Asia derived from geologic fault rates, Journal of Geophysical Research: Solid Earth, 101, 27943–27956, https://doi.org/10.1029/96JB02698, 1996.
- Prentice, C. S., Kendrick, K., Berryman, K., Bayasgalan, A., Ritz, J. F., and Spencer, J. Q.: Prehistoric ruptures of the Gurvan Bulag fault, Gobi Altay, Mongolia, Journal of Geophysical Research: Solid Earth, 107, ESE 1-1-ESE 1-18, https://doi.org/10.1029/2001JB000803, 2002.
 - Ramel, F., Ritz, J.-F., Ferry, M., Malcles, O., Davaasambuu, B., Arzhannikova, A. V., Arzhannikov, S., Chebotarev, A., Danzansan, E., Ayush, D., Munkhuu, U., and Demberel, S.: Inframillimetric slip rate and ∼8kyr long recurrence intervals for Mw ≥ 7.5 earthquakes along the southern section of the Har-Us-Nuur fault (Mongolian Altay), BSGF, https://doi.org/10.1051/bsgf/2025001, 2025.
 - Ritz, J. F., Brown, E. T., Bourlès, D. L., Philip, H., Schlupp, A., Raisbeck, G. M., Yiou, F., and Enkhtuvshin, B.: Slip rates along active faults estimated with cosmic-ray-exposure dates: Application to the Bogd fault, Gobi-Altaï, Mongolia, Geology, 23, 1019–1022, https://doi.org/10.1130/0091-7613(1995)023<1019:SRAAFE>2.3.CO;2, 1995.
- Ritz, J.-F., Bourlès, D., Brown, E. T., Carretier, S., Chéry, J., Enhtuvshin, B., Galsan, P., Finkel, R. C., Hanks, T. C., Kendrick, K. J., Philip, H., Raisbeck, G., Schlupp, A., Schwartz, D. P., and Yiou, F.: Late Pleistocene to Holocene slip rates for the Gurvan Bulag thrust fault (Gobi-Altay, Mongolia) estimated with 10Be dates, Journal of Geophysical Research: Solid Earth, 108, https://doi.org/10.1029/2001JB000553, 2003.
 - Ritz, J.-F., Vassallo, R., Braucher, R., Brown, E. T., Carretier, S., and Bourlès, D. L.: Using in situ–produced ¹⁰Be to quantify active tectonics in the Gurvan Bogd mountain range (Gobi-Altay, Mongolia), in: In Situ-Produced Cosmogenic Nuclides and Quantification of Geological Processes, Geological Society of America, https://doi.org/10.1130/2006.2415(06), 2006.
- Rizza, M., Ritz, J. -F., Prentice, C., Vassallo, R., Braucher, R., Larroque, C., Arzhannikova, A., Arzhannikov, S., Mahan, S., Massault, M., Michelot, J. -L., Todbileg, M., and ASTER Team: Earthquake Geology of the Bulnay Fault (Mongolia), Bulletin of the Seismological Society of America, 105, 72–93, https://doi.org/10.1785/0120140119, 2015a.





- Rizza, M., Ritz, J.-F., Prentice, C., Vassallo, R., Braucher, R., Larroque, C., Arzhannikova, A., Arzhannikov, S., Mahan, S.,
- 570 Massault, M., Michelot, J.-L., Todbileg, M., and ASTER Team: Earthquake Geology of the Bulnay Fault (Mongolia), Bulletin of the Seismological Society of America, 105, 72–93, https://doi.org/10.1785/0120140119, 2015b.
 - Sengor, A. M. C., Natalin, B., and Burtman, V.: Evolution of the Altaid Tectonic collage and Palaeozoic Crustal Growth in Eurasia, Nature, 364, https://doi.org/10.1038/364299a0, 1993.
- Shao, Y., He, J., Wang, X., and Zhao, Y.: Viscoelastic stress change from the 1931 MW7.8 Fuyun earthquake and its impacts on seismic activity around the Altai mountains, Geodesy and Geodynamics, 15, 326–337, https://doi.org/10.1016/j.geog.2024.01.002, 2024.
 - Tapponnier, P. and Molnar, P.: Active faulting and cenozoic tectonics of the Tien Shan, Mongolia, and Baykal Regions, Journal of Geophysical Research: Solid Earth, 84, 3425–3459, https://doi.org/10.1029/JB084iB07p03425, 1979.
- Tapponnier, P., Peltzer, G., Le Dain, A. Y., Armijo, R., and Cobbold, P.: Propagating extrusion tectonics in Asia: New insights from simple experiments with plasticine, Geology, 10, 611–616, https://doi.org/10.1130/0091-7613(1982)10<611:PETIAN>2.0.CO;2, 1982.
 - Thatcher, W.: Microplate model for present-day deformation of Tibet, J. Geophys. Res, 112, https://doi.org/10.1029/2005JB004244, 2007.
- Vassalo, R.: Chronologie et évolution des reliefs dans la région Mongolie-Sibérie: Approche morphotectonique et 585 géochronologique, 2006.
 - Vernant, P.: What can we learn from 20years of interseismic GPS measurements across strike-slip faults?, Tectonophysics, 644–645, 22–39, https://doi.org/10.1016/j.tecto.2015.01.013, 2015.
 - van der Wal, J. L. N., Nottebaum, V. C., Stauch, G., Binnie, S. A., Batkhishig, O., Lehmkuhl, F., and Reicherter, K.: Geomorphological Evidence of Active Faulting in Low Seismicity Regions—Examples From the Valley of Gobi Lakes, Southern Mongolia, Front. Earth Sci., 8, https://doi.org/10.3389/feart.2020.589814, 2021.
 - Walker, Nissen, E., Erdenebat, M., and Bayasgalan, A.: Reinterpretation of the active faulting in central Mongolia, Geology, 35, https://doi.org/10.1130/G23716A.1, 2007.
- Walker, Molor, E., Fox, M., and Bayasgalan, A.: Active tectonics of an apparently aseismic region: Distributed active strike-slip faulting in the Hangay Mountains of central Mongolia, Geophysical Journal International, 174, 1121–1137, https://doi.org/10.1111/j.1365-246X.2008.03874.x, 2008.
 - Walker, Wegmann, K. W., Bayasgalan, A., Carson, R. J., Elliott, J., Fox, M., Nissen, E., Sloan, R. A., Williams, J. M., and Wright, E.: The Egiin Davaa prehistoric rupture, central Mongolia: a large magnitude normal faulting earthquake on a reactivated fault with little cumulative slip located in a slowly deforming intraplate setting, Geological Society, London, Special Publications, 432, 187–212, https://doi.org/10.1144/SP432.4, 2017.
- Walker, R. T., Bayasgalan, A., Carson, R., Hazlett, R., McCarthy, L., Mischler, J., Molor, E., Sarantsetseg, P., Smith, L., Tsogtbadrakh, B., and Tsolmon, G.: Geomorphology and structure of the Jid right-lateral strike-slip fault in the Mongolian Altay mountains, Journal of Structural Geology, 28, 1607–1622, https://doi.org/10.1016/j.jsg.2006.04.007, 2006.





- Wang, M. and Shen, Z.-K.: Present-Day Crustal Deformation of Continental China Derived From GPS and Its Tectonic Implications, Journal of Geophysical Research: Solid Earth, 125, e2019JB018774, https://doi.org/10.1029/2019JB018774, 2020.
- Wang, Q., Zhang, Z., Freymueller, J., Bilham, R., Larson, K., Lai, X. A., You, X. Z., Zhijun, N., Wu, J., Li, Y. X., Liu, J., Yang, Z., and Chen, Q.: Present Day Crustal Deformation in China Constrained by Global Positioning System Measurements, Science (New York, N.Y.), 294, 574–7, https://doi.org/10.1126/science.1063647, 2001.
- Wang, W., Qiao, X., Yang, S., and Wang, D.: Present-day velocity field and block kinematics of Tibetan Plateau from GPS measurements, Geophysical Journal International, 208, 1088–1102, https://doi.org/10.1093/gji/ggw445, 2017.
 - Weldon, R. J., II, Fumal, T. E., Powers, T. J., Pezzopane, S. K., Scharer, K. M., and Hamilton, J. C.: Structure and Earthquake Offsets on the San Andreas Fault at the Wrightwood, California, Paleoseismic Site, Bulletin of the Seismological Society of America, 92, 2704–2725, https://doi.org/10.1785/0120000612, 2002.
- Windley, B. F., Alexeiev, D., Xiao, W., Kröner, A., and Badarch, G.: Tectonic models for accretion of the Central Asian Orogenic Belt, JGS, 164, 31–47, https://doi.org/10.1144/0016-76492006-022, 2007.
 - Wu, C., Huang, K., Yin, A., Zhang, J., Zuza, A. V., Haproff, P. J., and Ding, L.: Tectonic geomorphology and Quaternary slip history of the Fuyun fault, southwestern Altai Mountains, central Asia, Geosphere, 20, 735–748, https://doi.org/10.1130/GES02737.1, 2024.
- Xiao, W., Huang, B., Han, C., Sun, S., and Li, J.: A review of the western part of the Altaids: A key to understanding the architecture of accretionary orogens, Gondwana Research, 18, 253–273, https://doi.org/10.1016/j.gr.2010.01.007, 2010.
 - Xiao, W., Windley, B., Sun, S., Li, J., Huang, B., Han, C., Yuan, C., Sun, M., and Chen, H.: A Tale of Amalgamation of Three Permo-Triassic Collage Systems in Central Asia: Oroclines, Sutures, and Terminal Accretion, The Annual Review of Earth and Planetary Sciences, 43, 16.1 to 16.31, https://doi.org/10.1146/annurev-earth-060614-105254, 2015.
- Xu, X., Sun, X.-Z., Tan, X., Li, K., Yu, G., Etchebes, M., Klinger, Y., Tapponnier, P., and Woerd, J.: Fuyun fault: Long-term faulting behavior under low crustal strain rate, Dizhen Dizhi, 34, 606–617, https://doi.org/10.3969/j.issn.0253-4967.2012.04.007, 2012.
 - Yuan, W., Carter, A., Dong, J., Bao, Z., An, Y., and Guo, Z.: Mesozoic Tertiary exhumation history of the Altai Mountains, northern Xinjiang, China: New constraints from apatite fission track data, Tectonophysics, 412, 183–193, https://doi.org/10.1016/j.tecto.2005.09.007, 2006.
- 630 Zelenin, E., Bachmanov, D., Garipova, S., Trifonov, V., and Kozhurin, A.: The Active Faults of Eurasia Database (AFEAD): the ontology and design behind the continental-scale dataset, Earth System Science Data, 14, 4489–4503, https://doi.org/10.5194/essd-14-4489-2022, 2022.
 - Zumberge, J. F., Heflin, M. B., Jefferson, D. C., Watkins, M. M., and Webb, F. H.: Precise point positioning for the efficient and robust analysis of GPS data from large networks, Journal of Geophysical Research: Solid Earth, 102, 5005–5017,
- 635 https://doi.org/10.1029/96JB03860, 1997.